

Homology modeling and protein-protein interaction studies of GAPDH from *Helopeltis theivora* and chitinase from *Pseudomonas fluorescens* to control infection in tea [*Camellia sinensis* (L.) O. Kuntze] plants[☆]

Muthusamy Suganthi^a, Hari Sowmya^b, Jagadeesan Manjunathan^a, Pasiyappazham Ramasamy^c, Muthu Thiruvengadam^{d,e}, Venkatramanan Varadharajan^f, Baskar Venkidasamy^{g,*}, Palanisamy Senthilkumar^{h,*}

^a Department of Biotechnology, Vels Institute of Science, Technology & Advanced Studies (VISTAS), Pallavaram, Tamil Nadu 600117, India

^b Department of Bioengineering, Vels Institute of Science, Technology & Advanced Studies (VISTAS), Pallavaram, Tamil Nadu 600117, India

^c Department of Prosthodontics and Implantology, Saveetha Dental College & Hospitals, Saveetha Institute of Medical and Technical Sciences (SIMATS), Saveetha University, Chennai, Tamil Nadu, 600077, India

^d Department of Applied Bioscience, College of Life and Environmental Science, Konkuk University, Seoul 05029, Republic of Korea

^e Center for Global Health Research, Saveetha Medical College, Saveetha Institute of Medical and Technical Sciences (SIMATS), Saveetha University, Chennai, 600077, India

^f Department of Biotechnology, PSG College of Technology, Peelamedu, Coimbatore, India

^g Department of Oral and Maxillofacial Surgery, Saveetha Dental College and Hospitals, Saveetha Institute of Medical and Technical Sciences (SIMATS), Saveetha University, Chennai, 600077, India

^h Department of Genetic Engineering, SRM Institute of Science and Technology, Kattankulathur, Tamil Nadu 603203, India

ARTICLE INFO

Keywords:

Tea plant
Helopeltis theivora
Chitinase
Homology modeling
Protein-protein interactions
Biotic control

ABSTRACT

Tea [*Camellia sinensis* (L.) O. Kuntze] is an important crop cultivated in all over the world. The main problem in tea cultivation is the attack by a bug called *Helopeltis theivora*. Many different strategies, such as the use of pesticides and insecticides, have been developed to prevent pest attacks on tea crops. However, most pesticides and insecticides are also hazardous to the environment. Therefore, biopesticides can be used as alternatives to chemical pesticides to prevent pest attacks on crops. Chitinase is an important biopesticide owing to its ability to prevent pest growth. Hence, this enzyme could be used to target *H. theivora* by attacking *C. sinensis*. The present study involved *in silico* docking and binding analysis of a chitinase from *Pseudomonas fluorescens* MP-13 with glyceraldehyde 3-phosphate dehydrogenase (GAPDH) from *H. theivora*. The secondary structures of chitinase and GAPDH were determined using SOPMA, and their three-dimensional structures were modeled using the Swiss model and validated using PROCHECK and Ramachandran plots. Chitinase and GAPDH were docked using HADDOCK docking software. Docking studies governed a HADDOCK docking score of -125.8, which showed good binding between the two proteins. The amino acid residues involved in binding were analyzed using PDBSUM and the final docked structure was visualized using PyMol. Furthermore, in molecular dynamics studies, the binding region between chitinase and GAPDH residues was intact and stable, and did not detach throughout the simulation duration. It is clearly evidenced that chitinase from *P. fluorescens* and GAPDH from *H. theivora* interacted well with each other, thereby improves the chitinase's ability to target *H. theivora* and hence, chitinase can be used as a potent biopesticide. However, a detailed molecular functional and experimental studies are mandates to confirm the role of *P. fluorescens* in regulation of *H. theivora*.

Abbreviations: GAPDH, Glyceraldehyde 3-phosphate dehydrogenase; BLAST, Basic local alignment search tool; GRAVY, Grand average of hydropathicity; SOPMA, Self-optimized prediction method with alignment; HADDOCK, High ambiguity driven protein-protein docking; PDB, Protein data bank; RING, Residue interaction network generator.

[☆] This article is part of a special issue entitled: "Role of Microorganisms in Plant Growth, Stress Amelioration and Phytoremediation" published at the journal *Plant Stress*

* Corresponding authors.

E-mail addresses: baskarbt07@gmail.com (B. Venkidasamy), mpsenthilkumar@gmail.com (P. Senthilkumar).

<https://doi.org/10.1016/j.stress.2024.100377>

Received 27 November 2023; Received in revised form 11 January 2024; Accepted 28 January 2024

Available online 1 February 2024

2667-064X/© 2024 The Author(s). Published by Elsevier B.V. This is an open access article under the CC BY-NC-ND license (<http://creativecommons.org/licenses/by-nc-nd/4.0/>).

1. Introduction

Tea [*Camellia sinensis* (L.) O. Kuntze] is a perennial crop and the most popular beverage in the world (Samynathan et al., 2023a). It is one of the most important plantation crops in over 80 countries including Asia, Africa, and South America. Asia produces 89 percent of the global tea, while Africa produces nine percent (Samynathan et al., 2023a). *Helopeltis theivora*, a kind of mosquito bug, sucks the sap of tender shoots of *C. sinensis*, thus, severely affecting its growth and cultivation (Samynathan et al., 2023b; Bordoloi et al., 2023). Infection greatly affects plant growth and causes a 10–50 % reduction in productivity depending on the severity of the disease (Ranjithkumar et al., 2021). Artificial chemical pesticides can target *H. theivora*, but they can also produce harmful effects on *C. sinensis*, as well as on those who consume it. In addition, these chemical pesticides can damage soil, air, water, and environmental systems. Hence, a biological alternative for controlling *H. theivora* infections is of utmost importance. Many studies have demonstrated that enzymes are efficient biopesticides because of their ability to target pathogens and because they do not have any adverse effects on their hosts. Glycerinaldehyde 3-phosphate dehydrogenase (GAPDH) is an important enzyme in the biochemical pathway of *H. theivora* (Wang et al., 2019). Targeting this enzyme may be an important step in preventing mosquito bugs from destroying crops. Studies have shown that in malaria-causing mosquitoes, *Plasmodium* sporozoites contain GAPDH on their surfaces (Cha et al., 2016, 2021). Based on this hypothesis, GAPDH in *H. theivora* could be a target for preventing its effect on *C. sinensis*. Chitinase has long been used as a biopesticide (Iqbal and Anwar, 2019). Chitinase enters the gut of insects and causes significant damage to the peritrophic membrane by degrading chitin, preventing insects from feeding and resulting in death (Kramer and Muthukrishnan, 1997). In our previous study, we isolated chitinase from *Pseudomonas fluorescens* MP-13. The results of the investigation showed that *Pseudomonas fluorescens* is a great source of extracellular chitinase and that it completely killed *H. theivora* (Suganthi et al., 2017). In this study, chitinase was studied for the first time for its interaction with GAPDH isolated from *H. theivora*. Detailed molecular docking and dynamics studies were performed to determine the types of interactions and interacting residues as well as the binding stability between chitinase and GAPDH. Furthermore, preliminary *in silico* studies involving the binding analysis of chitinase and GAPDH were performed to test our hypothesis. The limitation of this study is that as an *in silico* computational approach is used to produce these results, biases may exist. To verify these findings, more *in vitro* research on the chitinase-GAPDH interaction is needed.

2. Materials and methods

2.1. Protein sequence and multiple alignments

The protein chosen for this study was GAPDH from *Helopeltis theivora*. The amino acid sequence of GAPDH (Accession ID: AOA5J6DQD0) was retrieved from the UniProt database (<https://www.uniprot.org/>). The suitable templates were identified using BLAST. Target templates were aligned using MAFFT Multiple sequence alignment. Finally, the homologous structure with the highest score was chosen as the template. In our previous study, we isolated chitinase from *Pseudomonas fluorescens* MP-13 (Suganthi et al., 2017). The isolated enzyme was purified, characterized, and sequenced. The sequence data were submitted to NCBI GenBank (ID: KM249884.1), which was then selected for binding analysis with GAPDH. Homologous templates were identified using BLAST. The templates were aligned using MAFFT, and a structure with a high alignment score was chosen as the template for modeling the chitinase structure (Katoh and Standley, 2013).

2.2. Physicochemical parameters, domain and secondary structure prediction

The physicochemical parameters of both GAPDH and chitinase sequences were predicted using ProtParam (<http://web.expasy.org/protparam/>). ProtParam is a web-based tool for determining the molecular weight, theoretical pI, amino acid composition, atomic composition, extinction coefficient, estimated half-life, instability index, aliphatic index, and grand average hydropathicity (GRAVY) of proteins (Gasteiger et al., 2005). The functional motifs in the proteins were determined using MOTIF (<https://www.genome.jp/tools/motif/>), a program used to identify the domains and motifs of a protein. The secondary structures of the modeled proteins were determined using SOPMA, an online web-based server available for predicting alpha helix and beta sheet structures in proteins (Geourjon and Deleage, 1995).

2.3. Homology modeling and refinement

The structures of GAPDH and chitinase were constructed based on homology modeling using the Swiss Model server (<https://swissmodel.expasy.org/#>). Energy minimization of the constructed models was performed using SwissPDB viewer (Guex and Peitsch, 1997). Finally, the refined structures were visualized using PyMol Molecular Viewer (DeLano, 2002).

2.4. Model validation

After energy minimization, the refined protein structures were evaluated using online validation tools to determine the model quality. The models were validated using the SAVES server, Ramachandran Plot, ERRAT, VERIFY3D, and PROVE programs (<https://saves.mbi.ucla.edu/>).

2.5. Docking and visualization

HADDOCK is a protein-protein docking software that performs flexible docking analysis of proteins. It is a host-friendly web-based docking tool available for free academic purposes. HADDOCK docking consists of three stages: (1) random orientation of atoms, (2) semi-flexible refinement, and (3) short flexible refinement format (Dominguez et al., 2003). After refinement, both the modeled structures of chitinase and GAPDH were submitted to the HADDOCK software. Ten clusters of docked positions of chitinase and GAPDH were determined using HADDOCK. Among them, based on the HADDOCK score and Z-value, that is, the standard deviation of atoms, the best structure was downloaded from the PDB. The network interactions between amino acids were initially determined using the Residue Interaction Network Generator (RING) software (Piovesan et al., 2016). The amino acids that formed hydrogen bonds, non-bonded interactions, and salt bridges were determined using PDBSum (Laskowski et al., 2018). Finally, the docked conformations were visualized using PyMol Molecular Viewer (DeLano, Bromberg, 2004).

2.6. Molecular dynamics simulation

The stability of the chitinase – GAPDH complex was assessed by subjecting the complex to molecular dynamics simulations for 100 ns. Initially, the complex was simulated using Desmond v2022.1 within the Schrödinger suite, utilizing the output file obtained from the HADDOCK server in PDB format (Bowers et al., 2006). Prior to this simulation, the Maestro v13.1.137 protein preparation wizard was employed to refine the structure of the chitinase – GAPDH complex. This involves crucial steps such as assigning bond orders, adding hydrogen atoms, and forming disulfide bonds. For further refinement, restrained energy minimization was performed on the complex by employing OPLS-2005 force-field parameters within the Prime module of the Schrödinger suite.

The prepared protein complex was then immersed in a simple point charge (SPC) water model using the system builder module, defining specific system boundaries as cubic shapes with dimensions of 10 Å across all three coordinates (Wu et al., 2006). To neutralize the system, sodium and chloride counter ions were added, maintaining a salt concentration of 0.15 M. Electrostatic interactions and periodic boundary conditions were calculated using the particle mesh Ewald (PME) method (Kawata and Nagashima, 2001).

Subsequent MD simulations were conducted under specific conditions: temperature of 300 K, pressure of 1 atm, and thermostat relaxation time of 200 ps in the isothermal isobaric ensemble (NPT). The Nose–Hoover thermostat and the Martyn–Tobias–Klein barostat approaches were utilized to maintain temperature and pressure, respectively (Kumar Singh and Silakari, 2019). Trajectories were recorded every 4.8 ps during the 100 ns production run. After the simulation, various analyses were performed using the trajectory file. These analyses included computing the root mean square deviation (RMSD), root mean square fluctuation (RMSF), radius of gyration (Rg), polar surface area (PSA), solvent-accessible surface area (SASA), and the number of hydrogen bonds formed between chitinase and GAPDH over the course of the simulation. Additionally, advanced analyses, such as principal component analysis (PCA), dynamic cross-correlation matrix (DCCM) analysis, and free energy landscape (FEL) analysis, were conducted using the Bio3D package in R software (Grant et al., 2021) and the Geo measures plugin in PyMOL software (Kagami et al., 2020).

3. Results and discussion

3.1. Protein sequence and multiple alignments

The amino acid sequence for the GAPDH protein was retrieved in FASTA format from the UNIPROT database, and the chitinase sequence used in the present study was identified through sequencing analysis in our previous study. BLAST similarity search against the Protein Data Bank (PDB) database showed structurally homologous proteins for the target sequences. Two sequences with the maximum identity for each protein were chosen from the BLAST search and aligned with the target sequences using the MAFFT tool. Templates with maximum alignment were chosen to model the structures of the target proteins. For GAPDH, PDB ID: 6LGJ (Chain A) was chosen as the template, whereas PDB ID: 4AXN (Chain A) was chosen as the template for chitinase.

3.2. Physicochemical parameters, domain and secondary structure

The molecular weight of GAPDH protein was 35,612.90 Da and the theoretical PI was 8.51. The instability index of the protein was 18.28, suggesting that the protein was stable. The estimated half-life under in vitro conditions was 30 h, the aliphatic index was 90.72, and the GRAVY value was –0.066. These values were similar to those of a previous study on GAPDH isolated from domestic animals, in which the PI ranged between 8.2–8.5, the instability index was 18.22, and the aliphatic index was 84 (Sahoo et al., 2019). For chitinase, the molecular weight, pI, and instability index were 39,045.20 Da, 5.63, and 32.09, respectively, suggesting that it is a stable protein structure. A similar study on bacterial chitinase showed a slight variation in molecular weight, which was approximately 58,712.04 Da (Dutta et al., 2021). However, the pI value was 5.67, which was very similar to the pI of our protein. Table 1 lists the values of various physicochemical parameters of GAPDH and chitinase proteins. Any protein with an instability index less than 40 is considered stable (Guruprasad et al., 1990). Based on this hypothesis, both GAPDH and chitinase proteins evaluated here were found to be naturally stable. Motifs are small regions of amino acids in proteins with functional significance. Motifs are the signature of proteins and are highly conserved regions that are mostly associated with unique functions (Savojardo et al., 2023). The number of functional motifs in GAPDH and chitinase identified from the MOTIF Finder database were 3

Table 1

Physicochemical Parameters of Proteins computed using the ExPASyProtParam tool.

Physicochemical Parameters	GAPDH	Chitinase
AA length	333	354
Molecular weight	35,612.90	39,045.20
Theoretical pI	8.51	5.63
Ext. coefficient	31,525	69,330
Absorbance	0.885	1.776
Instability index	18.28	32.09
Aliphatic index	90.72	88.53
Half-Life	Hours	Hours
GRAVY	–0.066	–0.167

and 1, respectively. Figure S1 shows the functional motifs present in GAPDH and chitinase proteins.

From SOPMA analysis, the secondary structure of GAPDH showed 32.73 % alpha helix, 32.43 % random coil, 26.43 % extended strand, and 8.41 % beta turn as the major secondary structures (Figs. S2 & S3). Similar findings were found in a related study that used SOPMA to predict the secondary structure of GAPDH from ostriches. They revealed 32.65% alpha helices, 23.53 % extended strands, 35.00 % random coils (α - and β -turns), and 8.82 % β -turns (Tian et al., 2014). The secondary structure of chitinase showed 34.46 % alpha helices, 40.40 % random coils, 17.51 % extended strands, and 7.63 % beta turns as the major secondary structures. Figs. 2 and 3 show the secondary structures of the GAPDH and chitinase residues, respectively. Similar to our results, more random coils have been identified in the secondary structure of chitinase (Dutta et al., 2021).

3.3. Homology modeling and refinement

The models were constructed using the SWISS Modeler. Swiss Modeler is an automated protein structure modeling software that works on the principles of homology modeling. It is a user-friendly free software comprising four main steps in protein structure modeling: (i) identification of the template, (ii) alignment of the target and template structure, (iii) modeling of the protein structure, and (iv) evaluation of the model. The modeled structures of GAPDH and chitinase were energy-minimized using the SWISS-PDB Viewer. Energy minimization is an important step in correcting the distorted geometries of the modeled structure. Swiss-PDBViewer is a user-friendly interface that allows us to work with several proteins simultaneously. The structures of GAPDH and chitinase revealed the presence of an alpha helix and beta sheets. A study on *Staphylococcus aureus* GAPDH structure prediction using homology modeling revealed a mixture of alpha helices and beta sheets, similar to our results (Almehmadi, 2020). This study's anticipated structure for chitinase revealed a higher prevalence of α -helices and a lower number of β -sheets. Similarly, the tobacco worm *Munduca sexta* chitinase structure has deformed beta sheets and alpha helices (Huang et al., 2000). The modeled structures of GAPDH and chitinase after refinement are displayed in Figs. 1 and 2, respectively.

3.4. Model validation

The predicted structures of chitinase and GAPDH were validated using SAVES. Structure validation is the process of evaluating the quality of created models. SAVES is an online server that provides different tools, such as ERRAT, PROVE, PROCHECK, and VERIFY 3D, to determine the quality of the modeled structures. Ramachandran plot analysis of chitinase showed 90 % amino acids in the most favored region and no amino acids were found in the disallowed region, indicating the high quality of the chitinase structure. The additional allowed region of 8.9 % amino acids and 0.4 % amino acids was present in the generously allowed region, and no amino acids (0 %) were in the disallowed region. Another study on the structure of the Swiss-model-modeled

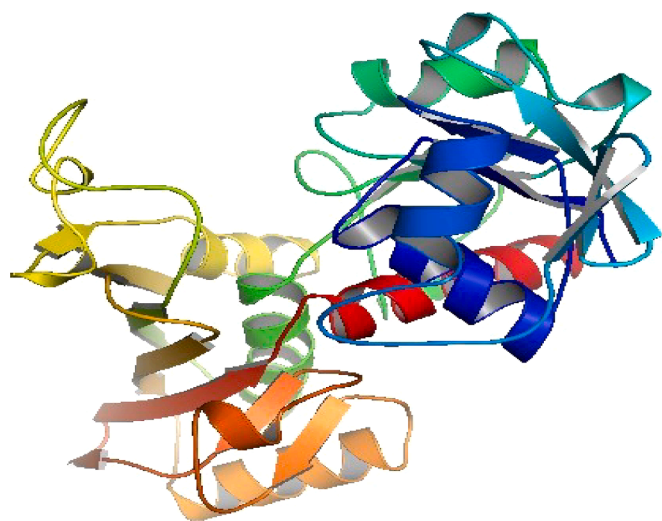


Fig. 1. Refined three-dimensional structure of GAPDH from *Helopeltis theivora*.

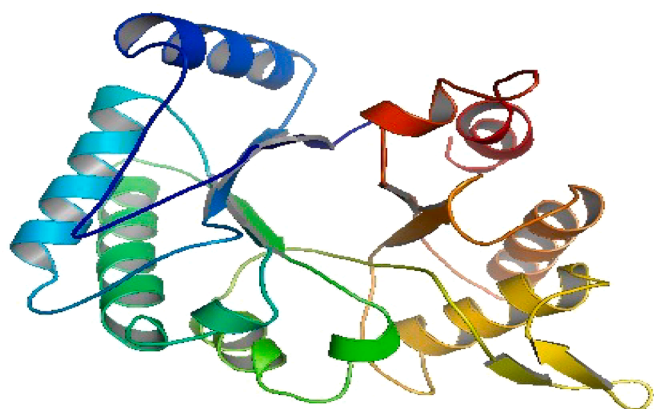


Fig. 2. Refined three-dimensional structure of chitinase from *Pseudomonas fluorescens* MP-13.

chitinase from *C. sinensis* had 84.8 % amino acids in the favored region, 14.3 % amino acids in the additional allowed region, and 0.4 % amino acids in the generously allowed and disallowed regions. The Verify3D results of our chitinase structure showed that at least 97.45 % of the amino acids had a 3D–1D score of >0.2 . Although the *C. sinensis* chitinase structure predicted by the researchers had 100 % amino acids with a 3D–1D score of >0.2 and the ERRAT score of their structures was very low at -91.003 (Chandra et al., 2017). ERRAT is the “overall quality factor” that determines the pattern of nonbonded atomic interactions in a protein. An ERRAT value >50 indicates good protein quality (Dhurigai et al., 2014). The ERRAT results of our chitinase structure showed an overall quality factor of 94.23 and from Verify 3D results, indicating a good quality model.

For GAPDH, the number of amino acids in the most favored region was 91.8 %. A previous study of the GAPDH structure and Ramachandran plot analysis revealed the presence of 87.5 % amino acids in the most favored region, 11.1 % amino acids in the favored region, 0.3 % amino acids in the generously allowed region, and 1.0 % amino acids in the allowed region. The overall quality factor for their structure from the ERRAT plot was 96.451, whereas it was 97.436 for our GAPDH protein structure (Rasal et al., 2016). From the Verify 3D results, it is clear that 97.89 % of residues in GAPDH had an average 3D–1D score >0.2 , suggesting that it is a good model. A probe plot was used to calculate the volume of atoms. It compares the volume of an atom with the standard atomic volume and gives a score based on any deviation from the

standard atomic volume. Figures S4 and S5 show the PROCHECK, PROVE, VERIFY 3D, and ERRAT results for the chitinase and GAPDH structures.

3.5. Docking

The modeled PDB structures of GAPDH and chitinase were submitted to the HADDOCK software. HADDOCK provided ten clusters of docked poses, among which the top score was highly reliable. Hence, the cluster with the highest score was analyzed and visualized using PyMol. The HADDOCK score for the top cluster was -125.8 and the Z-score was -1.9 . Z-score in the HADDOCK software is the standard deviation. A more negative Z-score suggested a better docked structure. Table 2 lists the score for HADDOCK docking analysis and the best docked pose was obtained from HADDOCK Server. The docked structure was analyzed with RING software to generate the contact maps of proteins. This generates residue pairs that are eligible for interactions. Figures S6 and S7 show the network of interacting residues in GAPDH and chitinase, respectively. The residues for protein-protein interactions were determined using PDBSum. After docking, the best structure was submitted to PDBSum to analyze the amino acid residues involved in protein-protein interactions. PDBSum clearly determined the number of hydrogen bonds, non-bonded interactions, salt bridges, and disulfide bond interactions between the atoms. Fig. 3 shows the number of bonding and non-bonding interactions between the chitinase and GAPDH. According to PDBSum results, the number of hydrogen bonds, salt bridges, and non-bonded interactions between chitinase and GAPDH were found to be 8, 2, and 99, respectively (Fig. 4). Fig. 3 shows the pores present in the docked structure after the interaction with GAPDH and chitinase. Finally, the predicted docked structure was visualized using PyMol (Fig. 5).

Another study on the HADDOCK score for *Zea mays* chitinase was -110 ± 2.1 , with RMSD (\AA) value of 27.4 ± 0.1 , Van der Waals score was $-63.4 \pm 4.0 \text{ kcal}\cdot\text{mol}^{-1}$, Electrostatic interaction was $-270.0 \pm 17.5 \text{ kcal}\cdot\text{mol}^{-1}$, Desolvation value was $5.9 \pm 1.4 \text{ kcal}\cdot\text{mol}^{-1}$, Restraints Violation Buried Surface Area (\AA^2) and 13.0 ± 19.2 and Z-score was $2103.7 \pm 17.7 -1.2$ involving glutamine, aspartic acid, proline, arginine, serine, threonine amino acids in the active site (Dowling, 2023). Additionally, as demonstrated by PDBSum, our structure includes these amino acids interacting with GAPDH through a variety of interactions, including disulfide bonds, salt bridges, hydrogen bonds, and non-bonded interactions.

3.6. MD simulation of chitinase–GAPDH complex

Fig. 6 illustrates the outcomes of the chitinase–GAPDH complex MD simulation, showing quantitative metrics including RMSD, RMSF, Rg, SASA, and PSA, which were measured throughout the simulation period. Fig. 6a shows the RMSD plot for both chitinase and GAPDH over a 100 ns MD simulation. RMSD evaluates the mean displacement between atoms within a molecular configuration in relation to a reference structure during the simulation period. It serves as a measure of the structural alterations within molecules, depicting the extent of atom movement or

Table 2

Results of docking scores predicted using HADDOCK.

Parameters	Value
HADDOCK score	$-125.8+/-1.8$
Cluster size	84
RMSD from the overall lowest-energy structure	$1.4+/-1.2$
Van der Waals energy	$-72.5+/-4.1$
Electrostatic energy	$-200.8+/-20.5$
Desolvation energy	$-35.3+/-3.4$
Restraints violation energy	$222.2+/-62.7$
Buried Surface Area	$2358.9+/-108.6$
Z-Score	-1.9

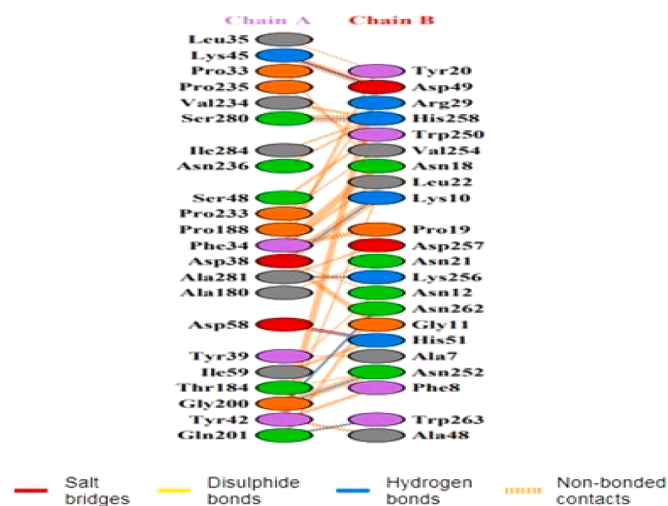


Fig. 3. The figure represents the residues involved in the interaction between GAPDH and chitinase; Chain A represents GAPDH; Chain B represents chitinase.

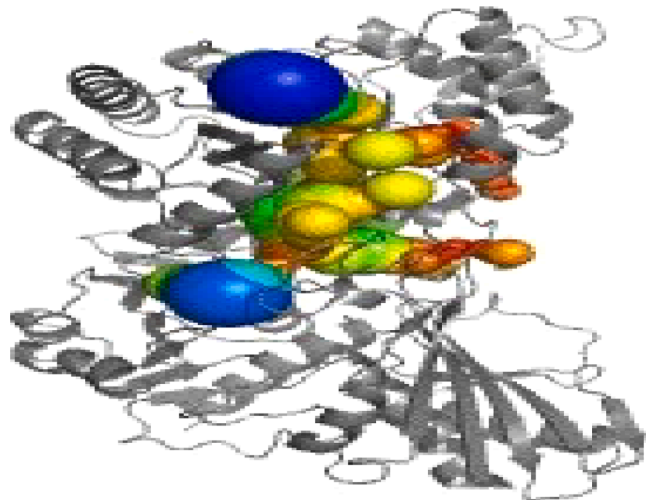


Fig. 4. PDBSum analysis of protein pores in the docked structure.

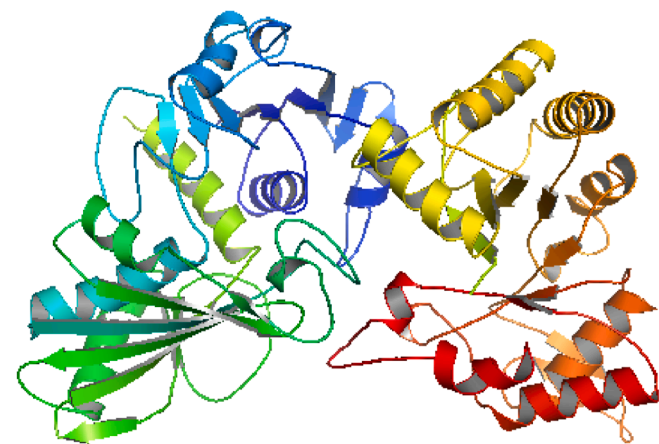


Fig. 5. Docked structure of GAPDH and chitinase visualized using PyMol.

deviation from their original coordinates (Wang et al., 2022). For GAPDH, the RMSD value steadily increased until reaching a maximum of 4.27 Å at 63 ns. Subsequently, it decreased, stabilizing at an average

of 3.5 Å for the remainder of the simulations. Conversely, chitinase exhibited a gradual increase in RMSD from the onset of the simulation, peaking at 3.75 Å at 60 ns. Following this peak, RMSD fluctuations stabilized, maintaining an average of 3.5 Å for the duration of the simulation. During the MD simulation, the average RMSD values for both GAPDH and chitinase were < 4 Å. This suggested minimal conformational changes in both proteins throughout the simulation period. Following RMSD computation, RMS fluctuations experienced by individual residues in the chitinase-GAPDH complex during the MD simulation were estimated, and the RMSF plots for GAPDH and chitinase are shown in Fig. 6b and c, respectively. Root Mean Square Fluctuation (RMSF) analysis involves assessing the average fluctuations of individual atoms or atom groups, such as residues, throughout a simulation. This metric is crucial for understanding the structural flexibility of the C α atoms within each residue in a given system (Haq et al., 2017). For instance, in the case of GAPDH, notable RMS fluctuations occurred in residues spanning from THR184 to LEU192. Among these, GLY190 exhibited particularly significant fluctuation, reaching an RMSF of 6.68 Å. In chitinase, the residues ILE221, ASN164, ALA214, ASN21, and GLY57 showed substantial RMS fluctuations, exceeding 3 Å. Interestingly, these residues, demonstrating high RMS fluctuation in both proteins, are situated within loop or coil regions that bridge secondary structures, such as α -helices and β -sheets. These fluctuations play a pivotal role in positioning the secondary structures, aiding the maintenance of interactions between chitinase and GAPDH during MD simulations. Additionally, it is noteworthy that among the residues displaying increased RMS fluctuations in both GAPDH and chitinase, certain residues were involved in these interactions. Consequently, some interactions between GAPDH and chitinase may not persist throughout the simulation.

The radius of gyration (Rg) serves as a pivotal measure in MD simulations, offering insights into the compactness and spatial arrangement of a molecular system by determining the average distance of particles from their collective center of mass (Filipe and Loura, 2022). In Fig. 6d, the alterations in Rg for both GAPDH and chitinase are illustrated over the course of MD simulation of the complex. The average Rg values recorded for GAPDH and chitinase throughout the MD simulation were found to be 20.88 Å and 19.4 Å, respectively. Notably, a slight increase in the Rg values for both proteins was observed during the simulation, indicating a gradual decrease in their compactness over time. This increase in Rg is primarily attributed to movements occurring within flexible regions of the proteins, such as loop regions, influenced by intermolecular interactions, solvent effects, or changes in chitinase-GAPDH contacts (Rahman et al., 2022). In addition to studying the radius of gyration (Rg), the solvent-accessible surface area (SASA) within the GAPDH-chitinase complex was assessed to quantify the extent of surface exposure to water molecules for both GAPDH and chitinase. Fig. 6e shows the variations in the SASA values of these proteins throughout the simulation. Notably, a marginal increase in SASA was noted for both proteins during the simulation, with GAPDH exhibiting a larger solvent-accessible area than GAPDH. The average SASA values recorded for chitinase and GAPDH within the complex were 14,370 Å² and 18,103 Å², respectively. Differences in the conformational dynamics and flexibility between chitinase and GAPDH could affect the exposed surface area. GAPDH may undergo more significant conformational changes or exhibit increased flexibility in certain regions than chitinase, resulting in a larger SASA (Lagzian and Ghanbarifardi, 2023). Next, the polar surface areas of GAPDH and chitinase proteins within the complex were calculated. This measurement was aimed at identifying the specific protein surface areas comprising polar or hydrophilic atoms/groups, including oxygen and nitrogen atoms engaged in hydrogen bonding or interactions with water molecules. Fig. 6f displays the PSA plot of chitinase and GAPDH during the MD simulation. Similar to SASA, a slight increase in PSA was observed for both proteins, with an average PSA of 7050 Å² for GAPDH and 6551 Å² for chitinase, during the simulation. Specific regions in proteins, such as loops or segments

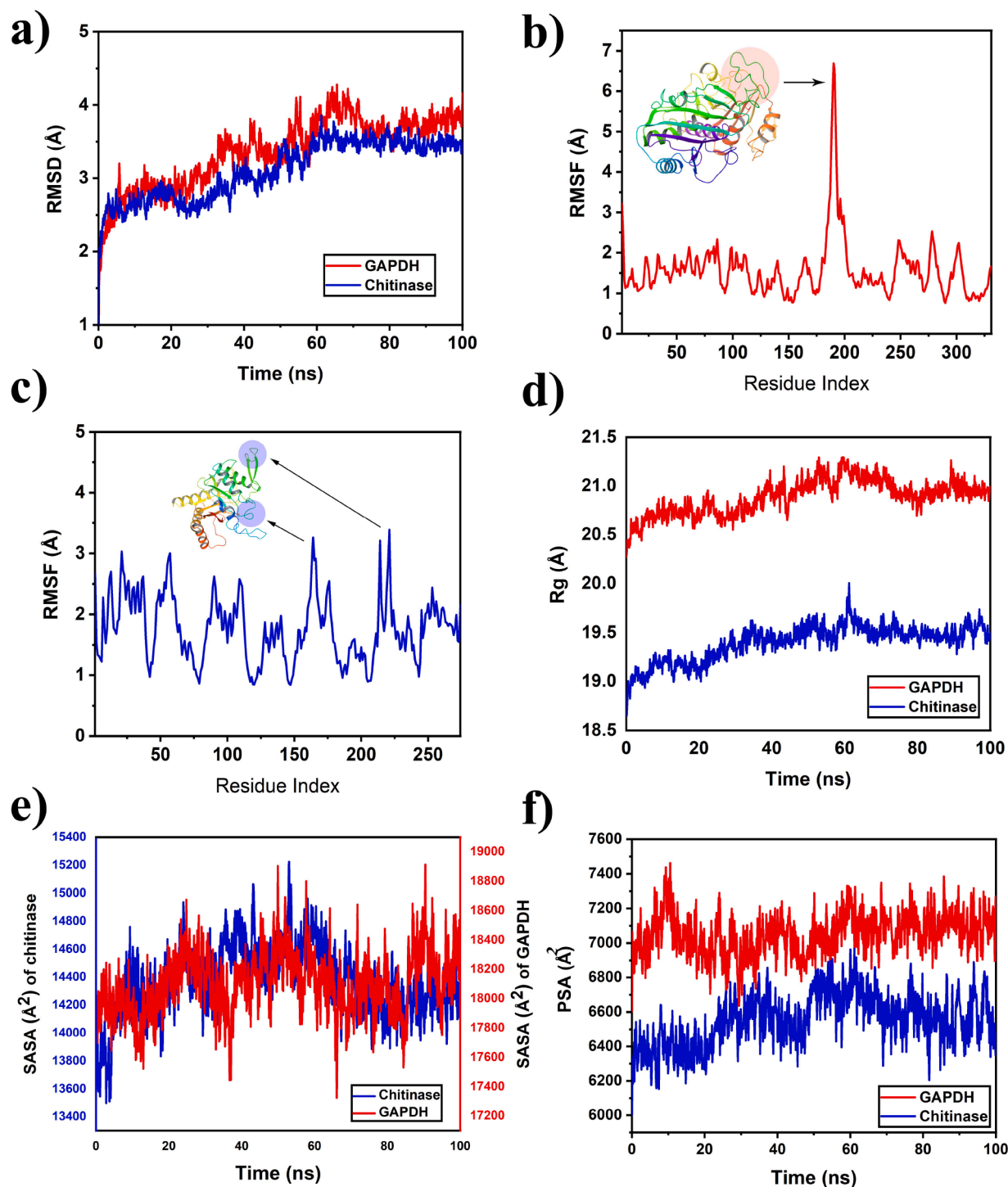


Fig. 6. The results of MD simulation of chitinase – GAPDH complex. a) Root mean square deviation plot, b) Root mean square fluctuation plot of GAPDH (red circles depicts regions of high RMS fluctuation), c) Root mean square fluctuation plot of chitinase (blue circles depicts regions of high RMS fluctuation), d) Radius of gyration plot, e) Solvent accessible surface area plot and f) Polar surface area plot.

containing polar residues, might transiently expose more surface area to solvent molecules, leading to an increase in the PSA.

The dynamics of the interaction between chitinase and GAPDH are shown in Fig. 7. Among the bonded interactions, hydrogen bonds play a significant role in mediating and stabilizing protein-protein interactions. Fig. 7a illustrates the formation of hydrogen bonds between chitinase and GAPDH over 100 ns. At the beginning of the simulation, approximately nine hydrogen bonds were observed, followed by a notable decrease in their number as the simulation advanced until reaching 20

ns. Subsequently, from 20 to 65 ns, the hydrogen bond count stabilized at around four, after which a gradual increase ensued, reaching a peak of 10 hydrogen bonds at 100 ns. The average number of hydrogen bonds observed during the simulation was 3.72. The increase in the number of hydrogen bonds formed towards the end of the simulation suggests a transition of the complex into a highly stable configuration (Jayaprakash et al., 2023). The conformational changes undergone by the complex during MD simulation were recorded as snapshots every 25 ns (Fig. 7b). The major conformational change observed during the

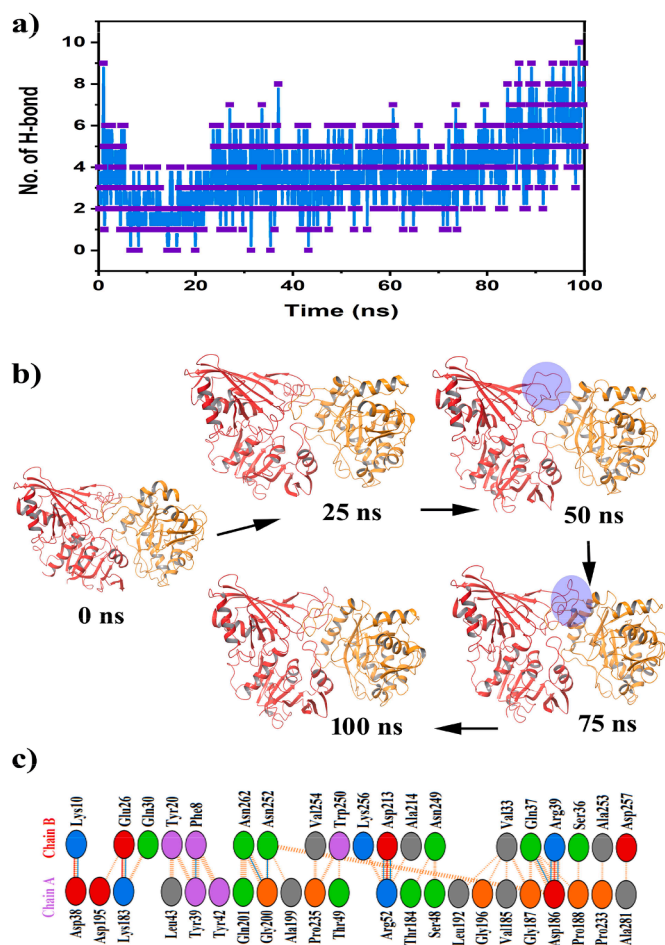


Fig. 7. The dynamics of interactions between chitinase and GAPDH during MD simulation. a) Hydrogen bond formation between chitinase and GAPDH over 100 ns simulation, b) snapshots of chitinase-GAPDH complex taken at 25 ns interval (blue color circles represents the areas of noticeable conformational change in the protein complex during simulation) and c) A 2D representation of various interactions between chitinase and GAPDH at 100 ns (Chain A – GAPDH, Chain B – chitinase, blue color line – hydrogen bond, red color line – salt bridge, yellow discontinuous lines – non-bonded interactions).

simulation of the chitinase-GAPDH complex was local unfolding of a highly flexible loop structure between THR184 and LEU192 in GAPDH (apparent in the snapshot taken at 50 ns). As the simulation progressed, the loop refolded at approximately 75 ns, achieving a more stable configuration that lasted until the end of the simulation. In addition, the transition from coils to transient helices was observed in chitinase throughout the simulation period. Regions that are initially disordered can transiently form helical structures because of short-lived stabilizing interactions (Patapati and Glykos, 2010). The aforementioned structural changes were consistent with the quantitative descriptors (RMSD, RMSF, Rg, and SASA) obtained during the simulation. Fig. 7c shows the bonded and non-bonded interactions between chitinase and GAPDH at 100 ns. A total of 10 hydrogen bonds, four salt bridges, and 93 non-bonded interactions were identified. Within GAPDH, the hydrogen bond-making residues include ASP38, TYR39, ARG52, LYS183, ASP186, and GLY200. Likewise, in chitinase, the hydrogen bond-forming residues identified were LYS10, PHE8, ASP213, GLU26, GLN37, ARG39, and ASN252. In contrast to the interactions noted at 0 ns, none of the initial interactions persisted throughout the simulation, primarily because most binding-site residues were situated in solvent-accessible loop regions. Despite the continuous alterations in the interactions between chitinase and GAPDH residues, the binding region remained intact, ensuring that the complex remained stable and did not detach

throughout the simulation duration.

3.7. PCA, DCCM and FEL analysis

Principal Component Analysis (PCA) was utilized to identify the alterations in the protein conformation due to the binding of GAPDH to chitinase, unveiling the combined motions observed within the MD trajectories (Ali et al., 2023). In PCA analysis applied to the MD trajectories of the GAPDH – chitinase complex, the atom coordinates of residues over time were structured into a matrix. Through centering and covariance computation, eigenvectors (principal components) are obtained, representing fluctuations in the structure of the complex. Projecting data onto these components facilitates the visualization of primary molecular motions or structural alterations during the simulation (Altis et al., 2007). Fig. 8 depicts the PCA plots generated from PC1, PC2, PC3, and the eigenvalues aligned with their respective eigenvector indices, illustrating the initial 20 modes of movement. The protein conformational shifts throughout the simulation were visualized as distinct clusters in PCA analysis. Blue clusters denote the most substantial movements, whereas white and red clusters signify intermediate and restricted motions, respectively. Eigenvectors, particularly the most common ones, serve as primary indicators of conformational alterations in the protein. In the case of GAPDH, the top five eigenvectors collectively account for 43.6 % to 75.2 % of the eigenvalues (Fig. 8a). For chitinase, these top eigenvectors covered 39.5 % to 75.2 % of the eigenvalues (Fig. 8b). Meanwhile, in the chitinase – GAPDH complex, the leading eigenvectors covered 33.9 % to 80.3 % of the eigenvalues (Fig. 8c). Higher percentages associated with specific eigenvectors indicate their capability to capture a more significant portion of the variance or dynamics within protein structures, underscoring their importance in elucidating crucial motions or conformational changes in these molecular systems. Notably, PCA plots revealed substantial variability within the PC1 cluster, accounting for 43.64 % for GAPDH, 39.5 % for chitinase, and 33.86 % for the complex. In contrast, PC2 cluster showed comparatively less variability, constituting 11.56 % for GAPDH, 16.46 % for chitinase, and 16.93 % for the complex. The PC3 cluster exhibited the lowest variability, encompassing 5.8 % for GAPDH, 5.85 % for chitinase, and 10.73 % for the complex. The convergence of data points observed at PC3, coupled with its minimal variability, signifies that in contrast to the PC1 and PC2 clusters, the protein structure demonstrates higher stability and compactness within PC3 (Paris et al., 2014). Consequently, the complex formed by chitinase and GAPDH appears to be less compact than the individual proteins but maintains a relatively stable conformation.

Following PCA, DCCM analysis was conducted to identify inter-residual motion within the MD trajectory of the chitinase – GAPDH complex. Fig. 9a illustrates the dynamic cross-correlation map of the chitinase-GAPDH complex, where red signifies positively correlated movements between residues and blue denotes anti-correlated motions. The correlation strength between the residues ranged from 0.82–0.64. Notably, a high degree of correlation was observed between residues 250 and 300 of GAPDH and residues 89–119 of chitinase. Additionally, flexible loop residues in GAPDH (180–192) displayed positively correlated motions with residues 21–40 of the chitinase. The prevalence of numerous positively correlated movements in the DCCM plot suggests stable attachment between GAPDH and chitinase (Li et al., 2022). Finally, the free energy landscape of the chitinase – GAPDH complex was explored, and the results are shown in Fig. 9b. In the FEL analysis, 3D and 2D plots were constructed to examine the trajectory of free energy variations concerning the Root-Mean-Square Deviation (RMSD) and Radius of Gyration (Rg). In these plots, the height or color of each point denotes the free energy level associated with a specific molecular configuration. Lower points or blue regions signify energetically favorable or stable conformations, whereas higher points or red regions indicate higher energy or less stable states. The energetically stable conformation of the chitinase-GAPDH complex, with a Gibbs free

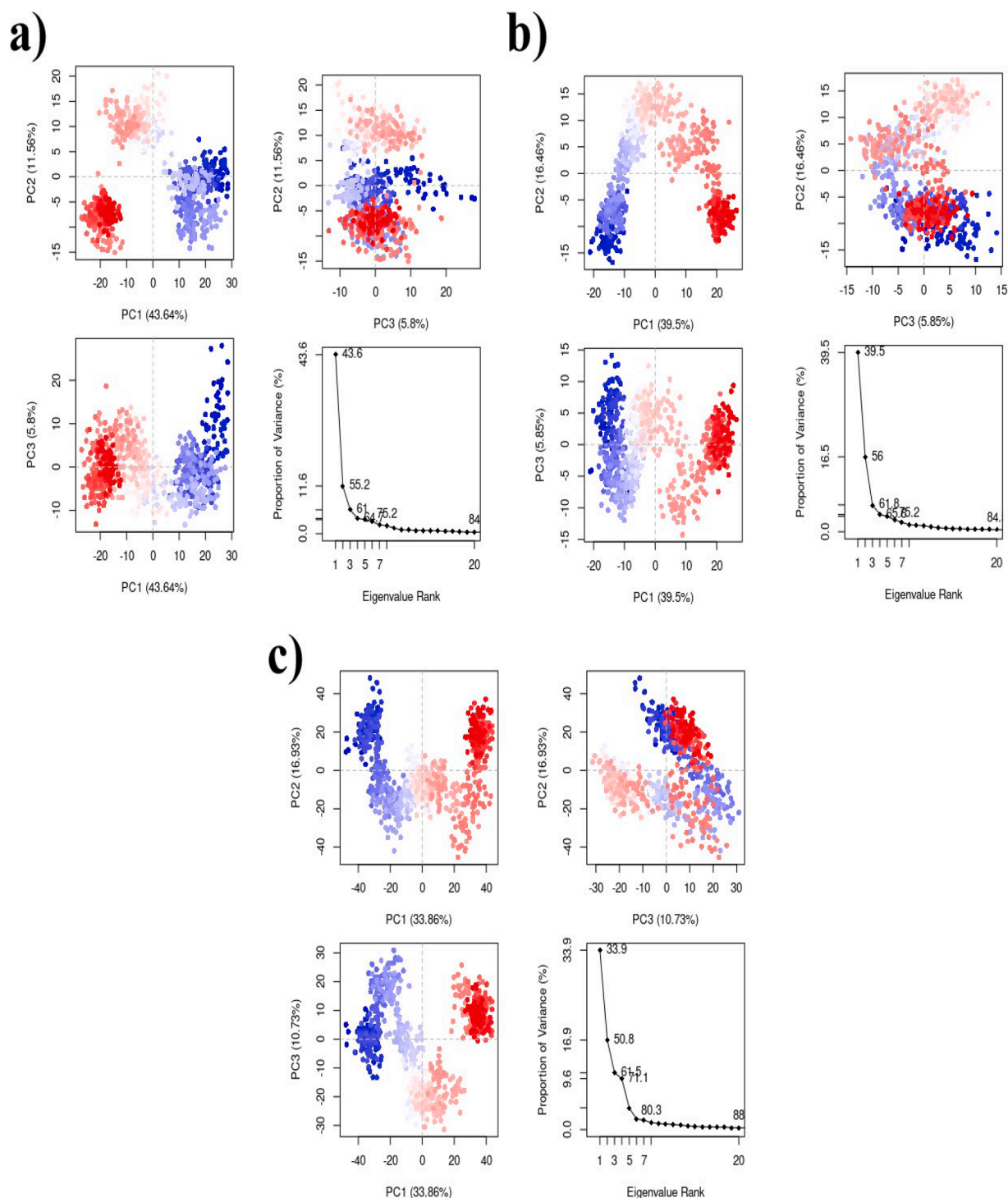


Fig. 8. Principal component analysis of MD trajectories of chitinase – GAPDH complex. a) PCA plots of GAPDH, b) PCA plots of chitinase and c) PCA plots of chitinase-GAPDH complex.

energy of 0 kJ/mol, was identified at an RMSD of 0.39 nm (3.9 Å) and an Rg of 2.79 nm (27.9 Å) (Fig. 9c). This stable conformation was observed during the latter part of the simulation period. Therefore, it can be inferred that before the end of the simulation, the chitinase-GAPDH complex attained an energetically stable conformation.

4. Conclusion

Protein-protein interactions affect the biological functions of proteins. This study reports an *in silico* analysis of chitinase and GAPDH

interactions using docking studies. Initially, the 3D structures of these two proteins were modeled and refined and their binding abilities were studied through docking. HADDOCK docking software was used to dock GAPDH and chitinase. The HADDOCK docking score was -125.8 . PDBSum was used to evaluate the amino acid residues involved in binding, and PyMol was used to visualize the final docked structure. Docking results revealed that both proteins formed hydrogen and other bonds, indicating their interaction. Based on these results, we concluded that GAPDH of *H. theivora* and chitinase of *P. fluorescens* could interact with each other; hence, chitinase can be used to target *H. theivora*. The

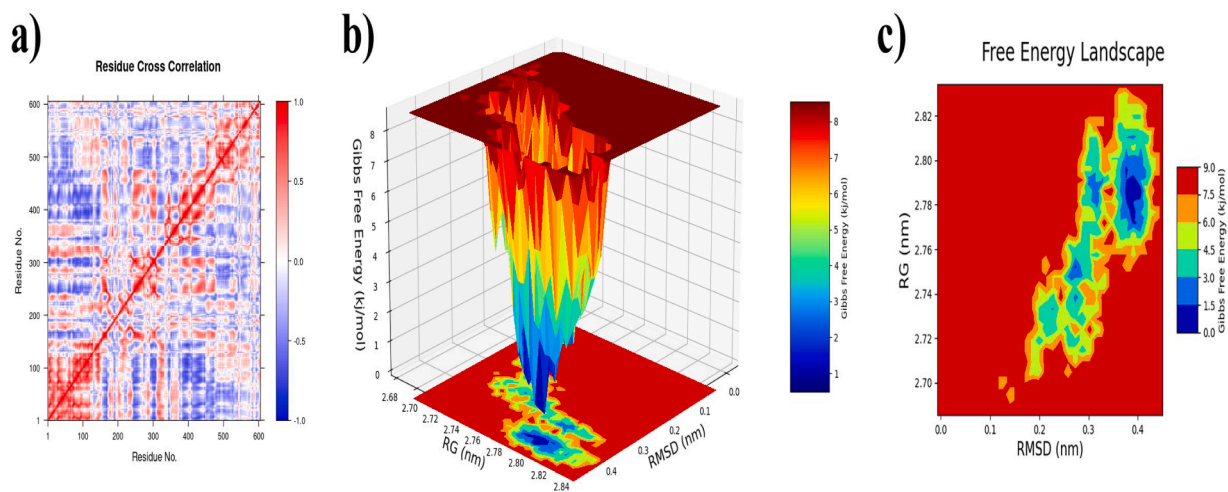


Fig. 9. DCCM and FEL analysis of chitinase-GAPDH complex. a) Dynamic cross-correlation map drawn between the residues of GAPDH (1 – 331) and chitinase (332 – 605), and b) A 3D and 2D representation of free energy landscape of chitinase-GAPDH complex.

interaction between chitinase and GAPDH is believed to improve the ability of chitinase to target *H. theivora*. Furthermore, detailed molecular dynamics studies emphasized that the interaction between chitinase and GAPDH was more stable and effective. Thus, our results suggest that *P. flourescens* chitinase is an efficient tool for controlling *H. theivora* infection in tea cultivation. However, this is a preliminary study involving in silico protein–protein interactions; further detailed molecular functional and experimental studies are required to confirm their biopesticide potential against *H. theivora*.

CRedit authorship contribution statement

Muthusamy Suganthi: Data curation, Conceptualization. **Hari Sowmya:** Formal analysis, Data curation. **Jagadeesan Manjunathan:** Methodology, Formal analysis. **Pasiyappazham Ramasamy:** Visualization, Software. **Muthu Thiruvengadam:** Writing – review & editing, Validation. **Venkatramanan Varadharajan:** Data curation, Formal analysis. **Baskar Venkidasamy:** Writing – original draft, Supervision. **Palanisamy Senthilkumar:** Conceptualization, Supervision.

Declaration of competing interest

The authors declare that they have no known competing financial interests or personal relationships that could have appeared to influence the work reported in this paper.

Data availability

Data will be made available on request.

Supplementary materials

Supplementary material associated with this article can be found, in the online version, at [doi:10.1016/j.stress.2024.100377](https://doi.org/10.1016/j.stress.2024.100377).

References

- Ali, I., Rasheed, M.A., Cavalu, S., Rahim, K., Ijaz, S., Yahya, G., Popovicu, M.S., 2023. Identification of natural lead compounds against hemagglutinin-esterase surface glycoprotein in human coronaviruses investigated via MD simulation, principal component analysis, cross-correlation, H-Bond Plot and MMGBSA. *Biomedicines*. 11 (3), 793.
- Almeahadi, S., 2020. Structure-function analysis glyceraldehyde-3-phosphate dehydrogenase homologue GapB in *Staphylococcus aureus*. *Int. J. Nature Life Sci.* 4 (2), 95–104.

- Altis, A., Nguyen, P.H., Hegger, R., Stock, G., 2007. Dihedral angle principal component analysis of molecular dynamics simulations. *J. Chem. Phys.* (24), 126.
- Bordoloi, K.S., Baruah, P.M., Agarwala, N., 2023. Identification of circular RNAs in tea plant during *Helopeltis theivora* infestation. *Plant Stress* 8, 100150.
- Ranjithkumar R., Kalaynasundaram M., Kannan M., Kennedy J.S., Chinnamuthu C.R., Paramaguru P. (2021). In vitro bio efficacy of botanicals against tea mosquito bug, *Helopeltis theivora* waterhouse in Tea.
- Bowers, K.J., Chow, E., Xu, H., Dror, R.O., Eastwood, M.P., Gregersen, B.A., Shaw, D.E., 2006. Scalable algorithms for molecular dynamics simulations on commodity clusters. In: *Proceedings of the 2006 ACM/IEEE conference on supercomputing*, pp. 84–es.
- Cha, S.J., Kim, M.S., Na, C.H., Jacobs-Lorena, M., 2021. Plasmodium sporozoite phospholipid scramblase interacts with mammalian carbamoyl-phosphate synthetase 1 to infect hepatocytes. *Nat. Commun.* 12 (1), 6773.
- Cha, S.J., Kim, M.S., Pandey, A., Jacobs-Lorena, M., 2016. Identification of GAPDH on the surface of Plasmodium sporozoites as a new candidate for targeting malaria liver invasion. *J. Exp. Med.* 213 (10), 2099–2112.
- Chandra, S., Dutta, A.K., Chandrashekara, K.N., Acharya, K., 2017. In silico characterization, homology modeling of *Camellia sinensis* chitinase and its evolutionary analyses with other plant chitinases. *Proc. Natl. Acad. Sci. India Section B* 87, 685–695.
- DeLano, W.L., 2002. Pymol: an open-source molecular graphics tool. *CCP4 Newsl. Protein Crystallogr.* 40 (1), 82–92.
- DeLano, W.L., Bromberg, S., 2004. *PyMOL User's Guide*. DeLano Scientific LLC, p. 629.
- Dhurigai, N., Daniel, R.R., Auxilia, L.R., 2014. Structure determination of leghemoglobin using homology modeling. *Int. J. Curr. Microbiol. App. Sci.* 3 (10), 177–187.
- Dominguez, C., Boelens, R., Bonvin, A.M., 2003. HADDOCK: a protein-protein docking approach based on biochemical or biophysical information. *J. Am. Chem. Soc.* 125 (7), 1731–1737.
- Dowling, N. (2023). A structural investigation of novel fungal polyglycine hydrolases.
- Dutta, B., Deska, J., Bandopadhyay, R., Shamekh, S., 2021. In silico characterization of bacterial chitinase: illuminating its relationship with archaeal and eukaryotic cousins. *J. Genetic Eng. Biotechnol.* 19, 1–11.
- Filipe, H.A., Loura, L.M., 2022. Molecular dynamics simulations: advances and applications. *Molecules*. 27 (7), 2105.
- Gasteiger, E., Hoogland, C., Gattiker, A., Duvaud, S.E., Wilkins, M.R., Appel, R.D., Bairoch, A., 2005. *Protein Identification and Analysis Tools On the ExPASy server*. Humana press, pp. 571–607.
- Geourjon, C.; Deleage, G., SOPMA: significant improvements in protein secondary structure prediction by consensus prediction from multiple alignments. *Comput. Appl. Biosci.* 11(6):681–4. [10.1093/bioinformatics/11.6.681](https://doi.org/10.1093/bioinformatics/11.6.681).
- Grant, B.J., Skjaerven, L., Yao, X.Q., 2021. The Bio3D packages for structural bioinformatics. *Protein Sci.* 30 (1), 20–30.
- Gue, N., Peitsch, M.C., 1997. SWISS-MODEL and the Swiss Pdb Viewer: an environment for comparative protein modeling. *Electrophoresis* 18 (15), 2714–2723.
- Guruprasad, K., Reddy, B.B., Pandit, M.W., 1990. Correlation between stability of a protein and its dipeptide composition: a novel approach for predicting in vivo stability of a protein from its primary sequence. *Protein Eng. Des. Sel.* 4 (2), 155–161.
- Haq, F.U., Abro, A., Raza, S., Liedl, K.R., Azam, S.S., 2017. Molecular dynamics simulation studies of novel β -lactamase inhibitor. *J. Mol. Graphics Model.* 74, 143–152.
- Huang, X., Zhang, H., Zen, K.C., Muthukrishnan, S., Kramer, K.J., 2000. Homology modeling of the insect chitinase catalytic domain–oligosaccharide complex and the role of a putative active site tryptophan in catalysis. *Insect Biochem. Mol. Biol.* 30 (2), 107–117.
- Iqbal, R.K., Anwar, F.N., 2019. Chitinases potential as bio-control. *Biomed. J. Sci. Tech. Res.* 14 (5), 10994–11001.

- Jayaprakash, P., Biswal, J., Pandian, C.J., Kingsley, J., Jeyakanthan, J., 2023. Investigation of translation initiation factor through protein–protein interactions and molecular dynamics approaches. *Mol. Simul.* 1–13.
- Kagami, L.P., das Neves, G.M., Timmers, L.F.S.M., Caceres, R.A., Eifler-Lima, V.L., 2020. Geo-Measures: a PyMOL plugin for protein structure ensembles analysis. *Comput. Biol. Chem.* 87, 107322.
- Katoh, K., Standley, D.M., 2013. MAFFT multiple sequence alignment software version 7: improvements in performance and usability. *Mol. Biol. Evol.* 30 (4), 772–780.
- Kawata, M., Nagashima, U., 2001. Particle mesh Ewald method for three-dimensional systems with two-dimensional periodicity. *Chem. Phys. Lett.* 340 (1–2), 165–172.
- Kramer, K.J., Muthukrishnan, S., 1997. Insect chitinases: molecular biology and potential use as biopesticides. *Insect Biochem. Mol. Biol.* 127 (11), 887–900.
- Kumar Singh, P., Silakari, O., 2019. In silico guided development of imine-based inhibitors for resistance-deriving kinases. *J. Biomol. Struct. Dyn.* 37 (10), 2593–2599.
- Lagzian, M., Ghanbarifardi, M., 2023. Tracing molecular adaptation of mudskippers from water to land transition: insight from the molecular dynamics simulation of collagen type-I. *Iranian J. Fisheries Sci.* 22 (2), 472–486.
- Laskowski, R.A., Jabłońska, J., Pravda, L., Varkova, R.S., Thornton, J.M., 2018. PDBsum: structural summaries of PDB entries. *Protein Sci.* 27 (1), 129–134.
- Li, M., Liu, X., Zhang, S., Liang, S., Zhang, Q., Chen, J., 2022. Deciphering the binding mechanism of inhibitors of the SARS-CoV-2 main protease through multiple replica accelerated molecular dynamics simulations and free energy landscapes. *Phys. Chem. Chem. Phys.* 24 (36), 22129–22143.
- Paris, G., Ramseyer, C., Enescu, M., 2014. A principal component analysis of the dynamics of subdomains and binding sites in human serum albumin. *Biopolymers* 101 (5), 561–572.
- Patapati, K.K., Glykos, N.M., 2010. Order through disorder: hyper-mobile C-terminal residues stabilize the folded state of a helical peptide. A molecular dynamics study. *PLoS. One* 5 (12), e15290.
- Piovesan, D., Minervini, G., Tosatto, S.C., 2016. The RING 2.0 web server for high-quality residue interaction networks. *Nucleic. Acids. Res.* 44 (W1), W367–W374. 19.
- Rahman, A., Saikia, B., Gogoi, C.R., Baruah, A., 2022. Advances in the understanding of protein misfolding and aggregation through molecular dynamics simulation. *Prog. Biophys. Mol. Biol.*
- Rasal, K.D., Chakrapani, V., Patra, S.K., Jena, S., Mohapatra, S.D., Nayak, S., Barman, H. K., 2016. Identification and prediction of the consequences of nonsynonymous SNPs in glyceraldehyde 3-phosphate dehydrogenase (GAPDH) gene of zebrafish *Danio rerio*. *Turkish J. Biol.* 40 (1), 43–54.
- Samynathan, R., Thiruvengadam, M., Nile, S.H., Shariati, M.A., Rebezov, M., Mishra, R. K., Venkidasamy, B., Periyasamy, S., Chung, I.M., Pateiro, M., Lorenzo, J.M., 2023a. Recent insights on tea metabolites, their biosynthesis and chemo-preventing effects: a review. *Crit. Rev. Food Sci. Nutr.* 63 (18), 3130–3149.
- Samynathan, R., Venkidasamy, B., Shanmugam, A., Khaled, J.M., Chung, I.M., Thiruvengadam, M., 2023b. Investigating the impact of tea mosquito bug on the phytochemical profile and quality of Indian tea cultivars using HPLC and LC-MS-based metabolic profiling. *Ind. Crops. Prod.* 204 (Part A), 117278.
- Sahoo, P.R., Mishra, S.R., Mohapatra, S., Sahu, S., Sahoo, G., Behera, P.C., 2019. In silico structural and phylogenetic analysis of glyceraldehyde 3-phosphate dehydrogenase (GAPDH) in domestic animals. *Indian J. Anim. Res.* 53 (12), 1607–1612.
- Savojardo, C., Martelli, P.L., Casadio, R., 2023. Finding functional motifs in protein sequences with deep learning and natural language models. *Curr. Opin. Struct. Biol.* 81, 102641.
- Suganthi, M., Senthilkumar, Arvinth, S., C, K.N., 2017. Chitinase from *Pseudomonas fluorescens* and its insecticidal activity against *Helopeltis theivora*. *J. Gen. Appl. Microbiol.* 63 (4), 222–227.
- Tian, Y.F., Li, H., Yuan, X.Y., Yang, Y.Z., Cui, B., 2014. Cloning and Characterization of Glyceraldehyde-3-Phosphate Dehydrogenase from Orchid (*Cymbidium goeringii*). *Asian Journal of Chemistry* 26 (17), 5321.
- Wang, Y., Parmar, S., Schneekloth, J.S., Tiwary, P., 2022. Interrogating RNA–small molecule interactions with structure probing and artificial intelligence-augmented molecular simulations. *ACS. Cent. Sci.* 8 (6), 741–748.
- Wang, Z., Meng, Q., Zhu, X., Sun, S., Gao, S., Gou, Y., Liu, A., 2019. Evaluation and validation of reference genes for quantitative real-time PCR in *Helopeltis theivora* Waterhouse (Hemiptera: Miridae). *Sci. Rep.* 9 (1), 13291.
- Wu, Y., Tepper, H.L., Voth, G.A., 2006. Flexible simple point-charge water model with improved liquid-state properties. *J. Chem. Phys.* 124 (2).